JOURNAL OF GEOPHYSICAL RESEARCH, VOL. 96, NO. A5, PAGES 7591–7601, MAY 1, 1991

Control of Plasma Waves Associated With the Space Shuttle by the Angle Between the Orbiter's Velocity Vector and the Magnetic Field

IVER H. CAIRNS AND DONALD A. GURNETT

Department of Physics and Astronomy, University of Iowa, Iowa City

The interaction between water outgassed from the space shuttle and the ionospheric plasma leads to production of water ions by charge exchange and an active and complex plasma wave environment for the space shuttle. We show that the amplitude and spectral character of some of these waves are controlled by the angle between the magnetic field and the shuttle's velocity vector $\mathbf{V}_T$ relative to the ionospheric plasma. When the flow is approximately perpendicular to the magnetic field ($V_\parallel/V_T \sim 0$), large wave amplitudes and characteristic "mushroom" wave structures are observed, whereas more nearly parallel flows $|V_\parallel| \sim V_\perp$ are characterized by low wave levels. We show that linear instability theory predicts the growth of Doppler-shifted lower hybrid waves in the observed frequency range when driven by the ring and/or beam distributions of water ions produced by charge exchange in the vicinity of the space shuttle. Two mutually compatible interpretations for the $V_\parallel/V_T$ effect exist. The first interpretation involves the path lengths available for growth of waves driven by pickup ions varying with the quantity $V_\parallel/V_T$ and being limited by spatial variations in the water ion distribution. The second interpretation follows directly from the linear theory: decreasing the ring/beam speed $V_\perp$ of the pickup ions driving the waves (increasing $V_\parallel/V_T$) results in smaller growth rates, with zero growth rate below some threshold value of $V_\perp$. The linear theory shows that decreased growth lengths or growth rates should naturally produce the observed amplitude and bandwidth changes constituting the $V_\parallel/V_T$ effect. These results have immediate implications for future shuttle missions and orbiting platforms subject to outgassing of water. If these facilities are used for ionospheric plasma studies or active experiments involving plasma waves, the plasma wave background due to pickup ions associated with the orbiter should be minimized. This requires orbits with large $|V_\parallel| \geq V_\perp$; that is, orbital velocities within about 45° of the magnetic field over as much of the orbit as possible. These constraints favor more nearly polar orbits and argue strongly against equatorial orbits. Alternatively, free-flying spacecraft situated upstream from the orbiter's water cloud should be used.

1. INTRODUCTION

Plasma measurements on the OSS 1, Spacelab 2, and other space shuttle missions have found the shuttle environment to be surprisingly active with high levels of several types of plasma waves [*Shawhan et al.*, 1984; *Murphy et al.*, 1983; *Hwang et al.*, 1987; *Gurnett et al.*, 1988], energetic particles [*Paterson and Frank*, 1989], multiple ion streams [*Stone et al.*, 1983], and many ionic and neutral species [*Narcisi et al.*, 1983; *Hunton and Calo*, 1985; *Grebowsky et al.*, 1987]. *Kurth and Frank* [1990] provide a recent review of the shuttle's plasma environment. The qualitative picture envisaged for the shuttle's interaction with the ionospheric plasma involves the steady outgassing of water vapor from the orbiter, the subsequent collisional charge exchange of these water molecules with ionospheric oxygen ions to form water ions, and the generation of plasma waves by "pickup" instabilities resulting from the different motions of the water ions and ambient plasma. Evidence exists for a cloud of neutral water surrounding the shuttle [*Carignan and Miller*, 1983; *Narcisi et al.*, 1983]. Water ions have been observed in the vicinity of the orbiter with the expected characteristics of the charge exchange process [*Paterson and Frank*, 1989]. The number densities of the water ions are qualitatively and often quantitatively consistent with theoretical models for the charge exchange process [*Paterson and Frank*, 1989; *Cairns*, 1990]. These number densities are substantial: $n_{H_2O^+}/n_{O^+} \geq 10\%$ within 10 m of the shuttle and $n_{H_2O^+}/n_{O^+} \sim 1\%$ within 100 m of the shuttle.

Paper number 90JA02564.
0148-0227/91/90JA-02564$05.00

This paper focuses on the observation and interpretation of plasma waves during the Spacelab 2 mission. The Spacelab 2 mission was launched on July 29, 1985, into a nearly circular, low-inclination orbit with an altitude of about 320 km and an inclination of 49.5°. One major objective of the mission was to investigate the shuttle–ionospheric plasma interaction at distances up to about 400 m from the orbiter. This study involved a small independent spacecraft, the Plasma Diagnostics Package or PDP spacecraft [*Shawhan*, 1982; *Kurth and Frank*, 1990], flying free of the shuttle during the so-called "free-flight" mission. The PDP spacecraft carried a full complement of particle and field instruments including a plasma wave receiver. This free-flight mission included two complete fly-arounds of the shuttle orbiter, as well as multiple traversals of the orbiter's plasma wake.

Previous work on the plasma waves associated with the space shuttle during the free-flight mission has been primarily directed toward explaining emissions generated by the FPEG experiment (fast pulse electron gun) [*Gurnett et al.*, 1986; *Bush et al.*, 1987; *Farrell et al.*, 1988; *Neubert et al.*, 1988; *Reeves et al.*, 1988] and describing the effects of thruster firings and magnetic conjunctions [*Gurnett et al.*, 1988]. Langmuir probe data have also been used to investigate low-frequency waves (below about 40 Hz) associated with water dumps and the shuttle's orbital maneuvering system and plasma wake [*Murphy et al.*, 1989; *Pickett et al.*, 1989; *Tribble et al.*, 1989, and references therein]. In this paper we will show that many of the variations in amplitude and spectral properties of the plasma waves from 31 Hz to 31 kHz observed well away from the shuttle during the free-flight mission, the so-called "mushroom" spectral features

to be discussed below, can be understood in terms of the variation of the angle between the orbiter's velocity vector relative to the plasma and the magnetic field vector, the so-called $V_\parallel/V_T$ effect. A linear theory is developed in which the waves are Doppler-shifted lower hybrid waves driven by pickup instabilities involving ring or beamlike distributions of water ions. Similar situations arise at comets [e.g., *Coroniti et al.*, 1986, and references therein] and with chemical release experiments [e.g., *Hudson and Roth*, 1988, and references therein]. The observed $V_\parallel/V_T$ effect is interpreted in terms of variations in both the path length available for wave growth and the growth rate of the pickup instability in response to orbital variations in $V_\parallel/V_T$. These results constitute a significant advance in the understanding of the plasma waves associated with the space shuttle. They also provide a criterion for design of future space shuttle missions, and the planned space station, in which minimizing the orbiter-associated plasma wave (and ion) background is important for passive and/or active space plasma investigations. To present these new results, this paper is organized as follows: the motions of charge-exchanged water ions and the background plasma particles are discussed in section 2, and the observational data are presented in section 3. Section 4 contains both an interpretation and a discussion of the observational results. A linear theory for generation of the plasma waves is developed in section 5. The implications of these works for design of future shuttle missions and the space station are discussed in section 6. The conclusions of the paper are given in section 7.

2. A Review of the Pickup Process

The coordinate system used in this paper, the so-called "pickup" system [*Cairns*, 1990] developed for studies of charge-exchanged water ions in the vicinity of the shuttle, moves with the space shuttle and is centered on the orbiter's center of mass. This reference frame (X_P, Y_P, Z_P) has the ionospheric magnetic field **B** along the Z_P axis. Without loss of generality the velocity of the background plasma may be written in the form $(-V_\perp, 0, -V_\parallel)$. Positive values of X_P then correspond to the region upstream from the shuttle. Motion of the background plasma across the magnetic field implies the existence of a self-consistent convection electric field $E = V_\perp B$ along the Y_P axis. A water ion born at zero velocity (the shuttle velocity) then moves in a cycloidal orbit in the X_P-Y_P plane with gyrospeed $V_\perp$ and gyrocenter velocity $(-V_\perp, 0, 0)$. Thermal motions lead to a distribution of gyrospeeds and gyrophases about this convection drift velocity $(-V_\perp, 0, 0)$ perpendicular to the magnetic field, as well as to a thermal distribution of gyrocenter drifts along the magnetic field (with zero average drift). In contrast, the ionospheric plasma particles have the same gyrocenter speed $V_\perp$ as the water ions in the X_P-Y_P plane, but have a gyrocenter drift speed $V_\parallel$ along the magnetic field. Plasma waves in regions where the water ions do not dominate the plasma convect with the ionospheric plasma. During the shuttle's orbital motion around the Earth, the angle between the velocity vector (relative to the ionospheric plasma) and the magnetic field varies from about 30° to 150°, where 90° corresponds to a velocity vector perpendicular to the magnetic field. Corotation of the ionospheric plasma is included when calculating the velocity of the ionospheric plasma relative to the shuttle orbiter; the plasma's corotation speed is of order 0.5 km s^{-1}, small compared to the orbital speed of order 7.8 km s^{-1}.

The space shuttle acts as an obstacle to the ionospheric plasma flow, resulting in the formation of a plasma wake behind the shuttle [*Murphy et al.*, 1989; *Tribble et al.*, 1989]. Since the wave data presented in this paper are primarily from the region downstream of the shuttle, we need to carefully consider the possibility that the observed plasma waves are associated with the wake rather than with pickup ions. The wake is expected to be centered directly behind the shuttle along the line of the shuttle's velocity vector (with respect to the ionospheric plasma). In the pickup coordinate system defined above, the expected center of the wake is at $Y_P = 0$ and $Z_P = X_P V_\parallel/V_\perp$. Positions relative to the expected wake center, and times of wake transits, can therefore be calculated and used to investigate the characteristics of any purely wake-associated plasma waves. For convenience here two new coordinates X' and Z' are defined by rotating the X_P-Z_P axes so that the X' axis is parallel to the plasma flow velocity and aligned along the center of the wake. That is, the expected center of the wake has coordinates $Z' = Y_P = 0$. Negative values of X' imply that the PDP spacecraft is a distance $|X'|$ downstream from the orbiter along the wake direction. Noting that the electron thermal speed (~200 km s^{-1}) greatly exceeds the shuttle's orbital speed (~8 km s^{-1}) and the ion thermal speed (~1 km s^{-1}), one expects that the magnetic field will influence the structure of the wake and make the Z' coordinate of the PDP a more sensitive indicator of position relative to wake structures than the Y_P coordinate. Wake transits are therefore defined below as transits $Z' = 0$ at small $Y_P \leq 10$ m. Plasma waves associated with the orbiter's plasma wake will be discussed elsewhere.

3. Observational Results

The data presented here are from the Helios subsystem of the plasma wave instrument on the PDP spacecraft [*Shawhan*, 1982; *Gurnett et al.*, 1988] and were obtained during the free-flight portion of the Spacelab 2 mission. The Helios instrument provides electric field measurements from 31.1 Hz to 178 kHz using 16 logarithmically spaced channels, four per frequency decade. A double-sphere antenna with a sphere separation of 3.89 m is used for detecting the electric fields during free flight. Each channel provides a data point every 1.6 s; only the peak signal during each measurement interval is used.

Plate 1 shows Helios data in a spectrogram format with wave amplitude color coded. The white curve at about 8 kHz shows the lower hybrid frequency computed using the square root of the electron to oxygen ion mass ratio times the electron gyrofrequency. There are three effects which complicate the interpretation of the data. First is the modulation at the spacecraft spin period of 13.6 s, most visible as a periodic blue spike in the spectrogram near 20 kHz, at all frequencies up to about 20 kHz. This modulation corresponds not to natural waves (the modulation period would be half the spacecraft spin period in this case), but to some presently unidentified source of spacecraft-associated interference. This effect leads to spurious signals during times of relatively low wave levels. The second interference effect is the impulsive production of intense waves by the orbiter's thrusters. These thruster signals are the yellow (typically)

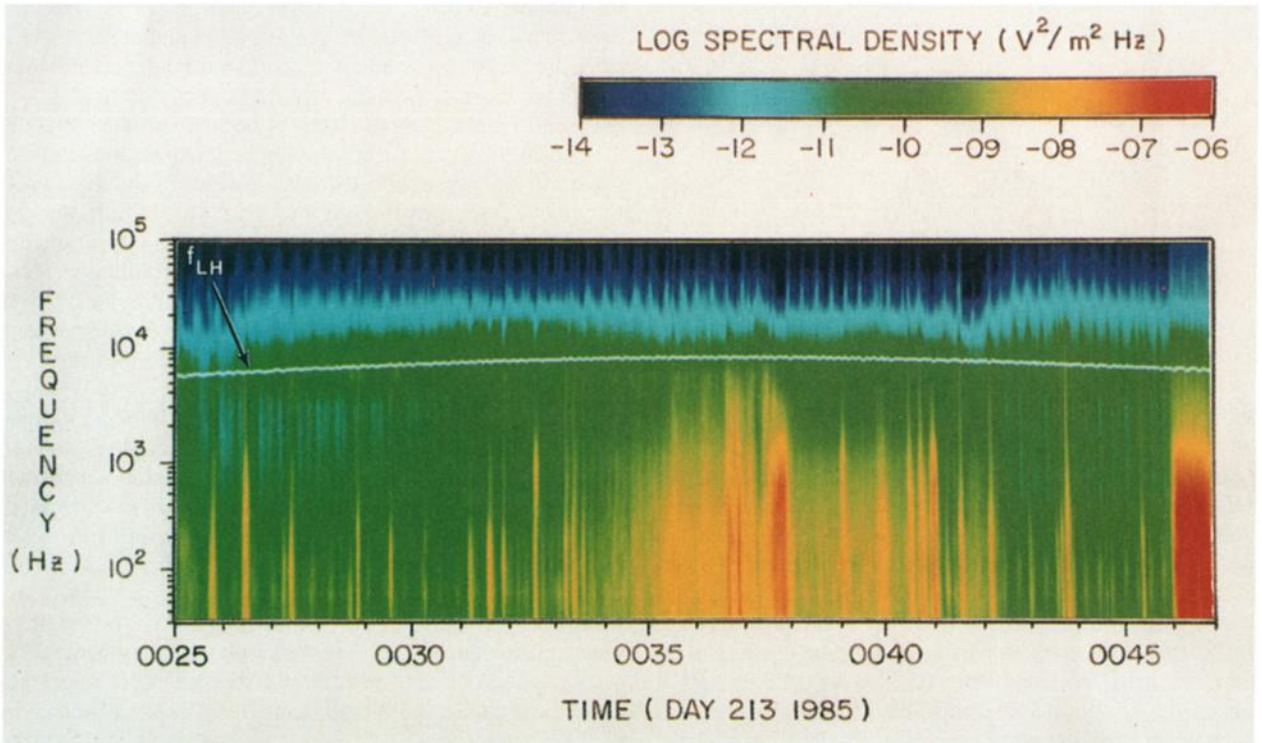

Plate 1. A frequency-time spectogram with color-coded amplitude for the period 0025–0047 UT, day 213, 1985, during the PDP's free-flight mission. The white curve shows the lower hybrid frequency. A "mushroom" spectral feature is seen between about 0031 and 0042. Wake transits occur near 0028, 0032, and 0041 with no accompanying changes in the wave spectrum.

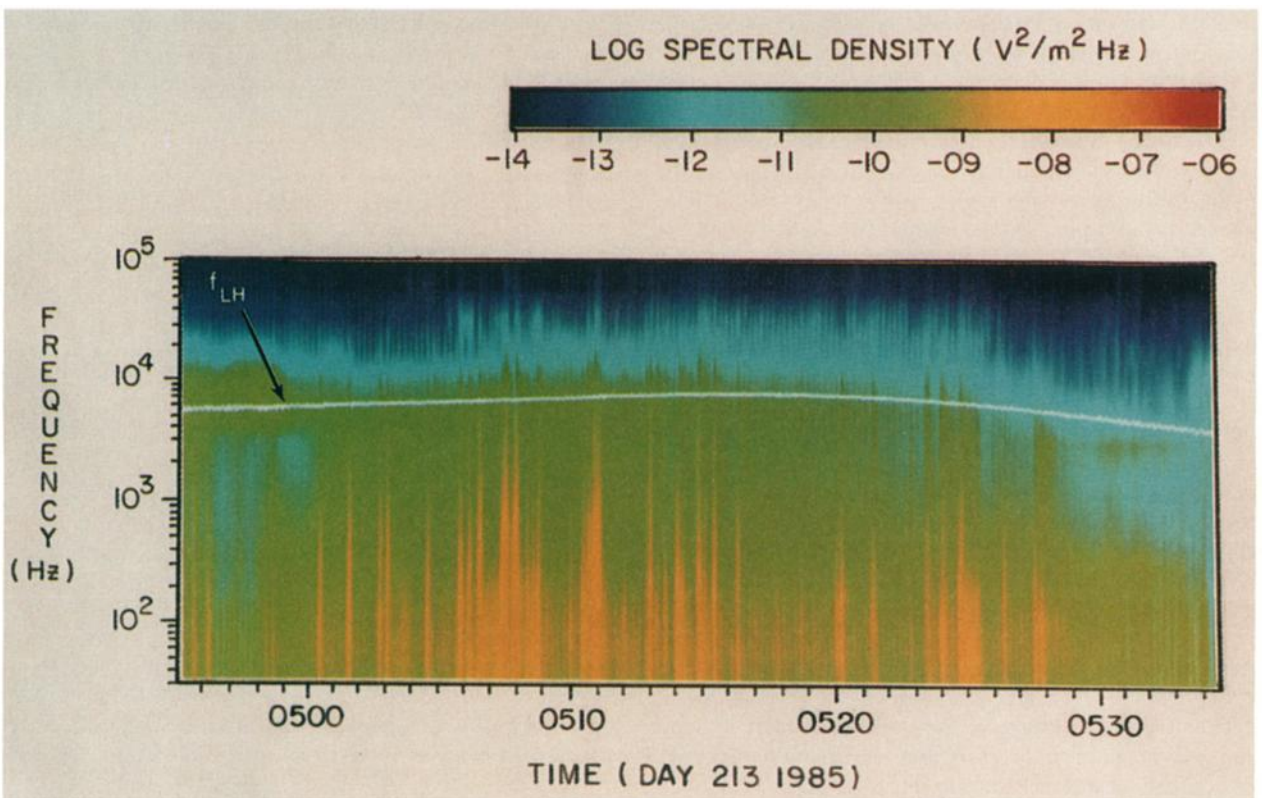

Plate 2. Another example of a "mushroom" spectral feature (in Plate 1's format) consistent with control of the waves by the parameter $|V_\perp/V_\parallel|$. Differences between this figure and Plate 1 indicate that position is not unimportant in determining the wave amplitude and detailed characteristics of the mushroom feature.

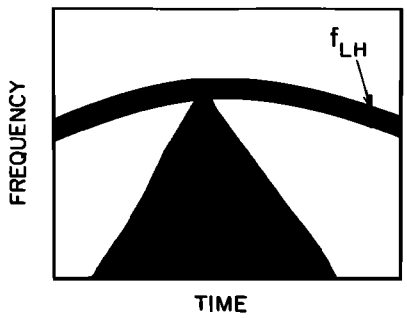

Fig. 1. An idealized "mushroom" spectral feature.

spikes which are most intense at low frequencies but extend up to about the lower hybrid frequency. Illustrative examples of these thruster signals, visible throughout this time period, occur at 0025:42, 0026:28, and 0037:40 (time format hour-minute:second; all times are universal time). Not all thruster firings result in intense, impulsive signals: the diffuse, relatively weak, broadband (up to f_{LH}) enhancement shown in Plate 1 from 0025:00 to about 0025:30 (but which starts at 0024:48) does correspond in time with almost continuous thruster firings from 0024:48 to 0025:05 and is almost certainly a thruster signal. Some thruster firings also produce no observable wave signals at the PDP spacecraft. All wave signals were therefore carefully checked against the record of thruster firings to eliminate thruster-associated waves from further consideration. No water dumps [e.g., *Pickett et al.*, 1989] occurred during the PDP free-flight mission. The third interference effect is that of the FPEG experiment, visible as the intense red signals from about 0046:10 to 0047:00 in Plate 1, with intense signals at all frequencies up to about 20 kHz together with signals near the electron gyrofrequency [*Gurnet et al.*, 1986; *Farrell et al.*, 1988].

The feature of interest in this paper is the "mushroom" spectral feature in Plate 1: the top of the mushroom is formed by the lower hybrid frequency waves, while the base is the triangular-shaped emission which starts at low frequencies and extends up to the lower hybrid frequency near the mushroom's center. This feature is illustrated schematically in Figure 1. This mushroom-shaped feature also corresponds to a significant and smooth (punctuated by thruster firings) enhancement in the intensity of the low-frequency waves by a factor of order 10. The time record of thruster firings shows that the smoothly varying mushroom feature is not due to the effects of thruster firings. For instance, the smooth enhanced wave levels (light yellow color) for the period 0038:00–0039:07 near the center of the mushroom feature are not associated with thruster firings: no thruster firings occurred from 0037:58 until 0039:07. Correspondingly, all the impulsive yellow and red signals in the data either correspond directly to the times of thruster firings or are associated with the modulated spacecraft interference pattern discussed above. The lower hybrid frequency waves show little evidence of change over the time period of the mushroom, except for frequency changes corresponding solely to variations in the magnetic field amplitude. Therefore the primary characteristics of interest are the increase in the frequency bandwidth of the triangular-shaped features (up to the lower hybrid frequency) and the smooth increase in amplitude of the low-frequency waves near the mushroom's apex. During the time period of Plate 1, the first "station-keeping" period, the PDP spacecraft is located in the wake region downstream from the shuttle and remains almost stationary relative to the shuttle's plasma wake (coordinates X', Y_P, and Z'), as shown in Figure 2. Wake transits occur near 0028:40, 0031:45, and 0041:15 with no accompanying changes in the plasma waves. This time period does, however, coincide with a transition from positive to negative values for $V_\parallel$. The quantity $V_\parallel/V_T$ passes through zero near 0037:00, coinciding with the maximum intensities of the low-frequency waves and the apex of the mushroom spectral feature. This feature in the plasma waves therefore apparently corresponds to variations in the quantity $V_\parallel/V_T$ and not to plasma waves associated purely with the orbiter's plasma wake.

Figure 3 shows the variation in the quantity $V_\parallel/V_T$ during the free-flight mission, giving the times of further predicted mushroom spectral features, the PDP's position relative to the orbiter at these times, and times of wake transits. Stylized mushroom features on the figure indicate where mushroom spectral features were indeed observed. In each case when the PDP was in the downstream region, mushroom spectral features were indeed observed to be centered near times when $V_\parallel/V_T = 0$, although the event near 0128 is somewhat problematical. While many of these mushroom features occur within a few minutes of transits of the center of the orbiter's wake, the events near 0037 and 0515 and the many wake transits not accompanied by mushroom features show that mushroom features are not associated with the orbiter's plasma wake. These mushroom spectral features are usually not as well defined as in the station-keeping period of Plate 1; most mushroom features occur while the PDP is moving significantly relative to the orbiter. Below, deviations from the idealized mushroom shape are interpreted in terms of PDP motion and spatial variations of the wave spectrum for a given value of $V_\parallel/V_T$.

A second example of a mushroom spectral feature is given

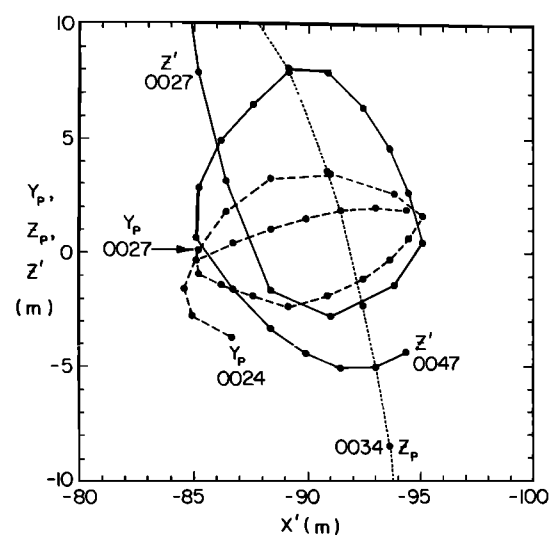

Fig. 2. The time variations in the PDP's coordinates Z', Y_P, and Z_P as a function of downstream position X_P for the period 0025–0047 using solid, dashed, and dotted lines, respectively. The solid circles are separated in time by 1 min. Noting the PDP's antenna length is approximately 4m, the PDP remains almost stationary relative to the orbiter's plasma wake (coordinates X', Y_P, and Z'). Wake transits occur near 0028, 0032, and 0041.

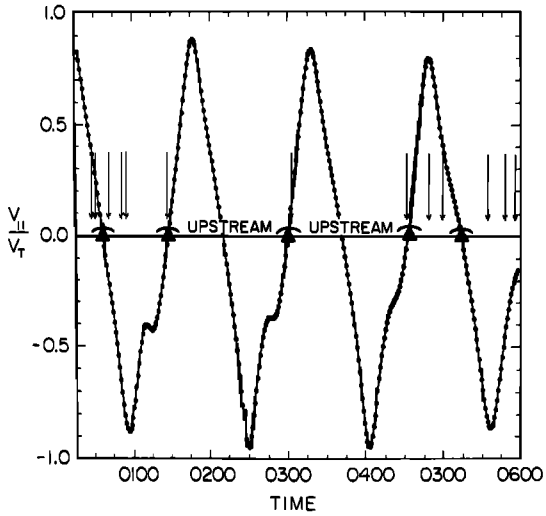

Fig. 3. The variation of $V_{\parallel}/V_T$ during the PDP's free-flight mission. Stylized mushrooms indicate where "mushroom" spectral features are observed, and arrows indicate transits of the center of the orbiter's wake. Times when $V_{\parallel}/V_T = 0$ and the PDP is not downstream from the orbiter are specified. Mushroom features are observed whenever $V_{\parallel}/V_T = 0$ and the PDP is downstream from the shuttle.

in Plate 2. The time scale extends from 0448 to 0536, with a mushroom spectral feature visible from about 0456 to 0530. Figure 4 shows the motion of the PDP spacecraft relative to the orbiter's plasma wake and the orbiter itself during this period. The PDP moves distances of order 50 m in all four coordinates shown, thereby implying significant motions relative to both the plasma wake and the orbiter during this time period. Wake transits take place at 0459 and 0534. These transits have no effects on the mushroom spectral feature. The quantity $V_{\parallel}/V_T$ passes through zero near 0514 and has a value greater than 0.5 from 0508 to 0520. These data are consistent with a mushroom spectral feature (1) occurring in conjunction with the variations in $V_{\parallel}/V_T$ and (2)

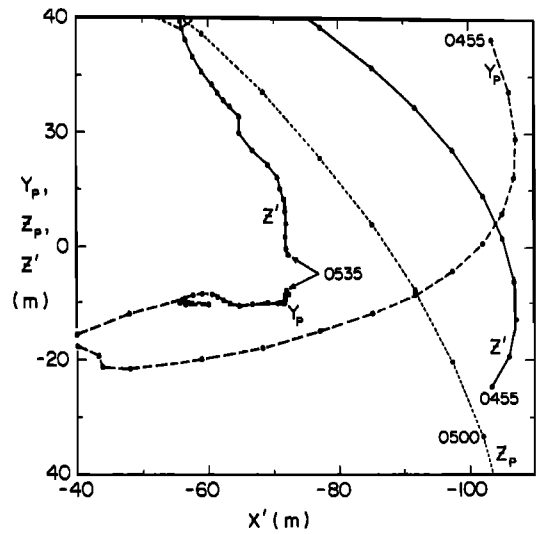

Fig. 4. The PDP's position relative to the orbiter for the period 0455–0535 in Figure 2's format. The PDP moves significantly relative to the orbiter's plasma wake. Wake transits occur near 0459 and 0534.

not being associated with specific structures in the orbiter's plasma wake. The differences between the events in Plate 1 and Plate 2 are interpreted in terms of the PDP's motion and of spatial variations in the wave characteristics in the orbiter's downstream region at constant $V_{\parallel}/V_T$.

4. Interpretation and Discussion of the Observations

We have shown that the so-called "mushroom" spectral features of plasma waves found downstream of the space shuttle orbiter during the Spacelab 2 mission are strongly correlated with the parameter $V_{\parallel}/V_T$: in particular the maximum amplitude, frequency bandwidth, and apex of a mushroom occur near where $V_{\parallel}$ goes through zero and the orbiter's velocity vector is perpendicular to the ionospheric magnetic field. We now argue that this correlation between mushroom spectral features and $V_{\parallel}/V_T$ has a natural interpretation in terms of the optimum conditions for wave growth driven by pickup water ions and the time available for evolution of the wave spectrum. Consider the growth of localized wave packets with sizes small compared with the water cloud (and water ion trail) and group velocities that lie in the X_P-Y_P plane and are small compared with the plasma flow velocity. (The argument below indicates that group velocities significantly out of the X_P-Y_P plane are inconsistent with the occurrence of the mushroom apexes near $V_{\parallel} = 0$.) These wave packets then move essentially with the background plasma through the water ion trail. When the orbiter moves perpendicular to the magnetic field, water ions produced by charge exchange of outgassed water molecules move in the same plane (the X_P-Y_P plane) and have the same gyrocenter velocity as the ionospheric plasma and the convected wave packets of plasma waves. Maximum path lengths for the growing waves, the maximum time for evolution of the wave spectrum, and a symmetry axis for the mushroom feature at $V_{\parallel} = 0$ can be envisaged in this case. In contrast, when the orbiter velocity has a significant component along the magnetic field, the pickup ions and the ionospheric plasma (and wave packets) move in different planes with significantly different gyrocenter velocities. The finite sizes of the orbiter's water cloud and water ion trail then imply a significant limitation of the growth length available for the waves. For instance, in a time equal to one ion cyclotron period a convected wave packet and a pickup water ion suffer a separation of order 250 sin α meters along the magnetic field, where α is the angle between the magnetic field and the plasma flow velocity, and a periodic separation of order 40 sin α meters in the X_P-Y_P plane due to the water ion gyromotion. In contrast, the characteristic scale of the water molecule cloud is of order 10–100 m in the high-density region of the cloud which might be expected to be the source region for the water ions driving the waves (i.e., pickup ion number densities in excess of 1%) [*Paterson and Frank*, 1989; *Cairns*, 1990], and the linear theory developed below predicts wavelengths of order 1–2 m. These strong spatial inhomogeneities in the water ion distribution function and number density imply considerable spatial variations in the dispersion relations of locally generated waves (as found, but not shown here, for the linear theory developed below) and so sensitivity to the effects of convection. There is therefore considerable scope for limitation of wave growth due to the different motions of the background plasma, plasma waves, and pickup ions. Here our intent is only to show the

plausibility of this mechanism for the observed $V_\parallel/V_T$ effect under a wide variety of unrestrictive conditions. Indeed, only slight modifications are necessary before this mechanism fits into the framework of the linear theory developed for the waves in the next section. In addition the linear theory for the waves also implies a separate, but compatible, mechanism for the $V_\parallel/V_T$ effect due to the nature of the pickup instability itself. We emphasize that the existence of the observed $V_\parallel/V_T$ effect is strong evidence that the waves are driven by water pickup ions.

Recent work on the plasma waves observed within 10 m of the space shuttle (called "near zone" waves here) during the XPOP roll (I. H. Cairns and D. A. Gurnett, Plasma waves in the near vicinity of the space shuttle, submitted to *Journal of Geophysical Research*, 1990; hereinafter Cairns and Gurnett, submitted manuscript, 1990; see also *Tribble et al.* [1989]) shows that the amplitude and spectral characteristics of the near zone plasma waves vary significantly with orbital variations in $V_\parallel/V_T$. Again, times with large $|V_\parallel/V_T| \geq 0.5$ show very low wave amplitudes. This provides further support for the observational results reported here.

The source region of the plasma waves forming the mushroom spectral features may be addressed as follows. In the first of two simple models the waves are generated throughout the region containing water ions produced from the orbiter's water cloud (this region might be referred to as the shuttle's water ion trail). In the second model the waves are generated within the near zone region of the orbiter and convected downstream. These models are not mutually incompatible, and both are plausibly consistent with the observed $V_\parallel/V_T$ effect. The first model permits the possibility that waves similar to the mushroom features might be observable when $|V_\parallel/V_T|$ is large during the PDP's two upstream excursions. Unfortunately, the PDP's path was not propitious for testing this possibility: both such time periods with $|V_\parallel/V_T| \geq 0.2$, 0206–0214 and 0338–0347, occurred at large Y_P or Z_P where small water ion number densities (and wave growth rates) are expected. (The absence of upstream waves during these times is not inconsistent with the linear theory developed in the next section.) The second model predicts that the waves should be observed only when downstream from or in the near vicinity of the space shuttle. Observational data [*Gurnett et al.*, 1988; *Tribble et al.*, 1989; Cairns and Gurnett, submitted manuscript, 1990] show that the intense near zone waves are strongly localized to the near vicinity of the space shuttle and are not convected downstream in recognizable form. Furthermore, the observed mushroom features show no well-defined variation in amplitude with downstream distance. These arguments suggest that the first source model for the waves is more consistent with the available data. However, further analysis of these wave data, as well as theoretical work on the models, is necessary before drawing firm conclusions on the source of the observed mushroom features. We note, moreover, that both models imply the possibility of significant spatial variations in the characteristics of both locally generated and convected waves, as appears necessary to understand the characteristics of the observed waves.

5. Linear Instability Theory Relevant to the Orbiter-Associated Waves

Theoretical calculations of the water ion distribution function in the vicinity of the space shuttle [*Cairns*, 1990] argue that the water ions have a ring distribution far from the orbiter, as observed by *Paterson and Frank* [1989]. However, with decreasing distance to the shuttle the water ion distribution function becomes increasingly well represented as a beam near zero velocity (superposed onto a ring with much lower number density). Both source models for the generation of the waves given in the last paragraph may therefore be discussed in terms of linear instabilities involving ring or beam distributions of water ions. In particular, the source model with wave growth throughout the water ion trail involves wave generation by primarily ringlike distributions of water ions [*Cairns*, 1990], while the second source model involves wave generation by primarily beamlike distributions of water ions. We now show that linear instability theory predicts that both ring and beam distributions of water ions should drive Doppler-shifted lower hybrid waves in the observed range of frequencies. A detailed development of the linear theory will be performed elsewhere; here we restrict our discussion to waves with wave vectors exactly perpendicular to the magnetic field, but note that calculations for wave vectors with components parallel to the field give similar results.

The electrostatic dispersion equation for plasma waves propagating exactly perpendicular to the magnetic field and observed in the shuttle frame may be written

$$1 - \frac{\omega_{pe}^2}{k_\perp^2 V_e^2} e^{-r_e^2} \sum_{m=-\infty}^{m=\infty} \frac{m\Omega_e}{\omega - k_x V_\perp - m\Omega_e} I_m(r_e^2) - \frac{\omega_{pO}^2}{k_\perp^2 V_O^2} e^{-r_O^2} \sum_{m=-\infty}^{m=\infty} \frac{m\Omega_O}{\omega - k_x V_\perp - m\Omega_O} I_m(r_O^2) - \frac{\omega_{pw}^2}{k_\perp V_\perp} \sum_{m=-\infty}^{m=\infty} \frac{2mJ_m(R_w)J_m'(R_w)}{(\omega - k_x V_\perp - m\Omega_w)} = 0 \quad (1)$$

In this equation the ionospheric electrons and oxygen ions are represented by magnetized Maxwellian distributions drifting with velocity $(-V_\perp, 0, 0)$ and have the standard forms for their contributions to the dispersion equation, while the water ions produced by charge exchange are represented by a magnetized delta function ring in perpendicular velocity (the functional form over parallel velocity is unimportant) [*Tataronis and Crawford*, 1970; *Hudson and Roth*, 1988, and references therein]. We restrict our attention to the case when the shuttle moves exactly perpendicular to the magnetic field. The functions J_m and I_m are the mth-order Bessel functions of the first and second kind, respectively. The arguments are $r_\alpha = k_\perp V_\alpha/\Omega_\alpha$ for the electrons and water ions, and $R_w = k_\perp V_\perp/\Omega_w$ for the water ions. Subscripts e, O, and w refer to the electrons, oxygen ions, and water ions, respectively. Standard definitions apply to the angular plasma frequencies $\omega_{p\alpha}$, gyrofrequencies Ω_α, and thermal speeds V_α for species α. Below, the water ions are also represented by an unmagnetized Maxwellian beam at zero velocity; in this case the sum over Bessel functions is replaced by the standard form involving the Fried-Conte function $Z(z_w)$ with $z_w = \omega/(2^{1/2}kV_w)$ and $k = k_\perp$ (by assumption). The dispersion equation is then

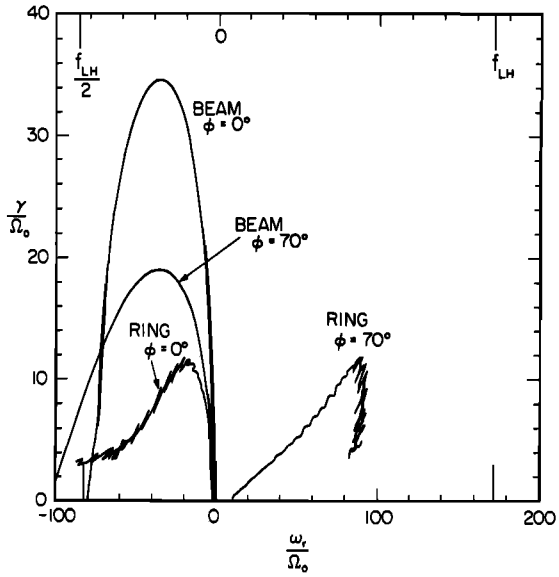

Fig. 5. Growth rates versus wave frequency for numerical solutions of equation (1) for both ring and beam distributions of water ions as marked. Curves are shown for two wave vector directions $\phi = 0°$ and $\phi = 70°$. Negative real frequencies result from Doppler-shifting, but only the magnitude of the wave frequency is directly observable. The plasma parameters are given in the text. The linear theory clearly predicts growth over the frequency bandwidth of the low-frequency component of the mushroom features.

$$1 - \frac{\omega_{pe}^2}{k_\perp^2 V_e^2} e^{-r_e^2} \sum_{m=-\infty}^{m=\infty} \frac{m\Omega_e}{\omega - k_x V_\perp - m\Omega_e} I_m(r_e^2)$$

$$- \frac{\omega_{pO}^2}{k_\perp^2 V_O^2} e^{-r_O^2} \sum_{m=-\infty}^{m=\infty} \frac{m\Omega_O}{\omega - k_x V_\perp - m\Omega_O} I_m(r_O^2)$$

$$+ \frac{\omega_{pw}^2}{k^2 V_w^2} [1 + z_w Z(z_w)] = 0 \qquad (2)$$

All quantities are defined in the "pickup" coordinate system described in section 2; in particular, the magnetic field defines the Z_P axis, and the X_P axis points upstream from the shuttle. Most important, however, is that the angular frequency ω is the frequency observable in the shuttle (or PDP) frame of reference. The quantity $\omega - k_x V_\perp$ is the Doppler-shifted wave frequency seen by the ionospheric electrons and water ions. A wave vector with a positive component k_x is directed upstream along the X_P axis. When solving this equation we normalize all quantities relative to those for the oxygen ions. Nominal ratios for the Spacelab 2 mission are $T_e/T_O = 2$, $T_w/T_O = 0.3$ (typically $T_O \sim 1000$ K), $V_\perp/V_O = 11$, and $\omega_{pO}/\Omega_O \sim 1000$ with an oxygen gyrofrequency of order 30 Hz. All frequencies calculated below are given in units of the oxygen gyrofrequency. In these units the nominal lower hybrid frequency f_{LH}, given by the square root of the electron to oxygen mass ratio times the electron gyrofrequency, is 172 units.

Figure 5 shows numerical solutions of the dispersion equation (1) for the growth rate as a function of the wave frequency ω_r for ring distributions of water ions, together with the analogous solutions when the water ions are represented as a beam centered at zero velocity. The relative water to electron number density is fixed at 5%. Curves are shown for two wave vectors in the X_P-Y_P plane: the $\phi = 0°$ curve corresponds to a wave vector directed upstream along the X_P axis. Linear theory clearly predicts that these particle distributions should drive waves from zero frequency to about the lower hybrid frequency with sizable growth rates. For all these solutions the waves with the maximum growth rates have positive frequencies near the lower hybrid frequency in the ionospheric plasma frame. The waves are therefore interpretable as Doppler-shifted lower hybrid–like waves. Strictly speaking, as described below, these waves do not lie on the lower hybrid mode; nevertheless, we follow standard practice [i.e., *Papadopoulos*, 1984] and refer to the waves as Doppler-shifted lower hybrid waves in the remainder of the paper. Negative values of ω_r in the shuttle frame result from Doppler-shifting of waves with frequency $\omega_{rest} \leq kV_\perp$ in the ionospheric plasma's rest frame. Note that only the absolute value of the wave frequency is observable.

More detailed comments on the waves driven by the ring distribution are as follows. In the ionospheric plasma frame the growing plasma waves form a series of flute modes with $\omega_{rest} \sim kV_\perp$ and maximum growth rates for wave frequencies near the lower hybrid frequency. These waves are similar to those of *Lee and Birdsall* [1979] in their "intermediate" and "strong ring" regimes. Only the dominant member of this series of modes is shown in Figure 5, i.e., mode "a" in Lee and Birdsall's Figure 5; this mode has the largest growth rate for a given wave frequency in the shuttle frame. For smaller ring densities this dominant mode breaks up into a forest of flute modes unstable over a limited range of wave frequencies, as hinted at by the series of jagged lines making up the ring-driven curves in Figure 5. Since the particle distribution functions are symmetric about zero velocity in the ionospheric plasma frame (corresponding to velocity $(-V_\perp, 0, 0)$ in the shuttle frame), the growth rates and frequencies of these flute modes in the ionospheric plasma frame do not depend on the angle ϕ; however, the Doppler shift, and so the wave frequency observed in the shuttle frame, does depend on ϕ. This Doppler shift moves the frequency of the maximum growth rate mode from near zero frequency for $\phi = 0°$ to near twice the lower hybrid frequency for $\phi = 180°$. Accordingly, linear theory implies that waves in the frequency range from zero frequency to several times the lower hybrid frequency could be generated by a ring distribution of water ions. The wavelengths of the growing modes should be of order 1–2 m, compared with the antenna length of 3.98 m.

A detailed discussion of the expected frequency spectrum of the waves requires careful consideration of both the angular dependence of the Doppler shift and the convective growth rate of the waves. In particular, even for a spectrum of waves with identical electric fields and wave numbers distributed uniformly over propagation angle ϕ, the cosine dependence of the Doppler shift on the angle ϕ concentrates the observed wave energy at $\phi = 0°$ and 180° [e.g., *Boardsen et al.*, 1990]. This effect would then lead to enhanced wave levels near zero frequency (i.e., $\phi \sim 0°$) and twice the lower hybrid frequency ($\phi \sim 180°$). The convective growth rates of these two peaks in the Doppler-shifted wave spectrum are quite different: in the shuttle frame the propagation speed (corresponding to the vector sum of the plasma convection velocity and the group velocity) of the upshifted plasma

waves near $2f_{LH}$ is $\sim 2V_\perp \sim 16$ km s^{-1} in the downstream direction, greatly exceeding that for the downshifted waves ($\sim 0.1V_\perp \sim 800$ m s^{-1}). Therefore, since the convective growth rate in the shuttle frame is given approximately by the temporal growth rate divided by the wave propagation speed, it is clear that the downshifted waves will grow much more effectively than the upshifted waves (a factor of 16 in convective growth rate). For the plasma described in Figure 5, the propagation/convection distance required for the waves to reach saturation (10 e-folding distances) is 4 m in the plasma frame, corresponding to 40 m in the shuttle frame. Detailed discussions of the distances available for effective wave growth must await development of a spatially inhomogeneous wave theory and comparison with theories for spatial variations in the water ion distribution function [cf. *Cairns*, 1990]. Qualitatively, however, the water ion distribution function is expected to show substantial spatial variations on the scale of the water ion gyroradius $V_\perp/\Omega_w \sim$ 40 m (for $V_\perp \gg V_\parallel$) in the shuttle frame. Distances of order 10–40 m (in the shuttle frame) are then sufficient for the above theory to predict the generation of significant levels, but not necessarily the saturation levels, of the downshifted waves. In this connection we note that the low-frequency waves in the mushroom features shown in Plates 1 and 2 have maximum energy densities of approximately 1–10 $\times$ 10^{-18} J m^{-3}. The ratios of wave energy density to water ion energy density and thermal plasma energy density are then approximately 10^{-9} and 3×10^{-10} (for $n_e = 10^{11}$ m^{-3}), respectively. These wave levels are therefore qualitatively consistent with the pickup instability not proceeding to saturation. In summary, the linear theory predicts that observable levels of the downshifted waves should grow at low frequencies in the shuttle frame, exactly as observed. At this stage, no interpretation of the lower hybrid frequency waves comprising the tops of the mushroom spectral features is apparent in terms of this theory.

A water ion beam centered at zero velocity, modeling the highly peaked beam arc distributions expected in the very near vicinity of the space shuttle [*Cairns*, 1990], may also drive rapidly growing waves at frequencies below the lower hybrid frequency as shown in Figure 5 (also Cairns and Gurnett, submitted manuscript, 1990). In fact, the ion beam produces larger growth rates (by a factor of order 3) than the ring distribution for the same number density of water ions. However, a ring distribution produces waves peaked at significantly lower frequencies, in better agreement with the observed waves. In the plasma rest frame the beam-driven waves have dispersion relations $\omega_{rest} \sim kV_\perp$ with maximum growth rates for wave frequencies near the lower hybrid frequency. The distribution of wave vectors is, however, different: waves driven by the ion beam are restricted to wave vectors with $\phi \leq 75°$, and also to negative real frequencies. The two curves show an extension to more negative frequencies with increasing angle ϕ, thereby potentially permitting an explanation involving linear theory for the increased frequency range of the observed low-frequency component of the "mushroom" spectral features. Again, no interpretation for the lower hybrid frequency waves in the mushroom features is apparent.

Two interpretations for the observed $V_\parallel/V_T$ effect are consistent with this linear theory. First, as suggested in section 4, coupling the different motions of pickup ions and convected wave packets with spatial inhomogeneity should

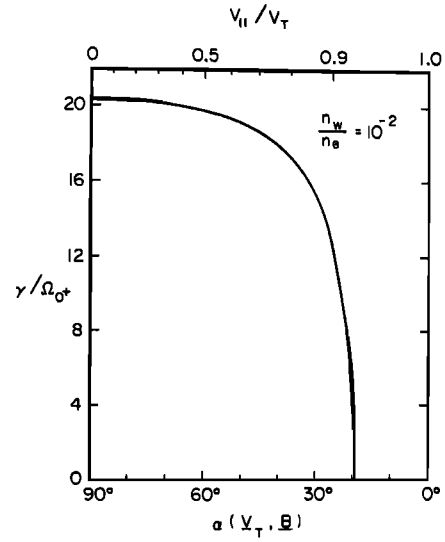

Fig. 6. Variation in the maximum growth rate for the beam-driven waves with the angle α (between $\mathbf{V}_T$ and $\mathbf{B}$) and the quantity $V_\parallel/V_T$. Significant growth requires $\alpha \geq 30°$ for a relative water ion beam density of 1%.

lead to growth lengths for the waves which vary with $V_\parallel/V_T$. Figure 5 then shows that increasing the growth length for the waves (decreasing $V_\parallel/V_T$) should lead naturally to enhancements in the wave levels, an increased range of wave vectors, and a greater frequency bandwidth for the observable waves. This is consistent with the observed amplitude-bandwidth correlation for the "low-frequency" component of the mushroom spectral features. The linear theory predicts that the observed waves should consist of wave packets elongated along the magnetic field that are convected downstream (in the shuttle frame), but with group speeds of order $0.9V_\perp$ antiparallel to the plasma flow velocity. The $V_\parallel/V_T$ argument in section 4 may be repeated without substantive changes with these specifications for the wave packets. Now, however, spatial variations in the water ion distributions and the characteristics of the locally growing waves are vital in limiting both the spatial extent of the wave packets along the magnetic field and the growth lengths of the waves: note, in particular, that separations along the magnetic field would have no effects on the growth length of ideal flute modes in an infinite homogeneous plasma (since the wave fronts are aligned along the magnetic field). Further discussion of this mechanism must await development of analytic theories or simulations that fully include spatially inhomogeneous wave growth and convection in a shuttle environment with more realistic water ion distributions [cf. *Cairns*, 1990]. Second, the ring speed $V_\perp$ driving the unstable waves decreases as the quantity $V_\parallel/V_T$ increases, thereby leading to a decrease in the amount of free energy available for wave growth and to decreases in the growth rate and frequency bandwidth of the waves. Similar effects are well known for ion acoustic instabilities [e.g., *Gary and Omidi*, 1987] and electron beam instabilities. Application of this idea to the shuttle environment is complicated by both the expected variation in the pickup ion number density with variations in $V_\parallel/V_T$ [*Cairns*, 1990] and the idealized (delta function) ring feature in the linear theory. Using a beam representation for the water ion distribution, Figure 6 shows

that the linear growth rate varies markedly with the quantity $V_\parallel/V_T$ and the angle α between the plasma velocity $\mathbf{V}_T$ and the magnetic field. In particular, when $\alpha \leq 30°$, very low path-integrated wave levels are expected. Calculations for ring distributions show similar results; however, due to the idealized delta function ring features used in this paper, significant growth occurs until $\alpha \leq 20°$. A realistic, thermally broadened ring is expected to have significantly lower growth rates than the delta function ring feature, implying that significant growth will only be possible for values of $V_\parallel/V_T$ smaller than or comparable to those for the beam.

The water ions produced near the space shuttle are expected [*Cairns*, 1990] to have characteristics intermediate to those of the pure ring and pure beam distributions described above. The linear theory discussed here predicts that both ring and beam distributions of water ions may drive Doppler-shifted lower hybrid waves in the range of observed frequencies (and observable wave numbers) for the low-frequency component of mushroom spectral features. Plausible means for producing the mushroom features (i.e., the $V_\parallel/V_T$ effect) are also apparent. At this stage, ring distributions appear to be more likely sources for the observed mushroom waves than beam distributions, based on (1) the ring instability producing waves at significantly lower frequencies than the beam instability, (2) the observed spatial localization and different characteristics of the near zone waves [*Tribble et al.*, 1989; Cairns and Gurnett, submitted manuscript, 1990], and (3) the natural interpretation of the near zone waves in terms of Doppler-shifted lower hybrid waves driven by beamlike distributions of water ions (Cairns and Gurnett, submitted manuscript, 1990). We note, however, that the effects of spatial inhomogeneity appear to be a vital ingredient for a complete theory for the waves and that nonlinear processes are often important, even dominant, in determining the evolution of the amplitude and frequency spectrum of plasma waves. Therefore further work on linear instability theory and computer simulations that address in detail the effects of spatial inhomogeneity are required to construct a detailed quantitative theory for the mushroom spectral features.

6. Implications for Future Space Missions in Low Earth Orbit

The role of the quantity $V_\parallel/V_T$ in controlling the amplitude and spectral characteristics of waves associated with the space shuttle may have important implications for the design of future missions involving orbital platforms subject to outgassing, such as the space shuttle or the proposed space station, which have a requirement that the background of plasma waves driven by outgassed pickup ions be minimized. This requirement for minimal levels of platform-associated plasma waves is a natural one for missions focused on either natural ionospheric plasma waves or active space plasma experiments involving plasma waves as either a diagnostic tool or the focus of the research. We note that both the plasma waves observed in the space shuttle's outgas cloud during the PDP free-flight mission (this paper) and the intense near zone plasma waves observed in the near vicinity of the space shuttle (Cairns and Gurnett, submitted manuscript, 1990; see also *Murphy et al.* [1983] and *Shawhan et al.* [1984]) show evidence of the $V_\parallel/V_T$ effect. Our comments therefore apply to both platform-based (i.e., the shuttle's payload bay) and free-flying experiments. Aside from the obvious comment that outgassing of potential pickup ions should be minimized, the primary implication of our observational research is that the platform's orbit should be designed so that $|V_\parallel| \geq V_\perp$. Both our theoretical interpretations imply that large values of $|V_\parallel/V_T|$ should be pursued. This means that polar orbits are strongly favored, whereas equatorial orbits are contraindicated.

We note, however, that a maximum value of $|V_\parallel/V_T|$ may exist: for $V_\perp = 0$ there is no convection electric field, and the pickup ions and background plasma once again move in the same plane, thereby again permitting more efficient wave growth. The pickup instability described in the last section has zero growth rate in this case; however, more familiar ion acoustic-type instabilities [e.g., *Gary and Omidi*, 1987] may grow in this case provided the temperature ratios T_e/T_O and T_O/T_w are sufficiently high. Therefore, in the absence of observational data with larger values of $|V_\parallel/V_T|$ than 0.95 during this shuttle mission, our primary recommendation is for future missions with a requirement for low levels of plasma waves associated with the orbiting platform to have orbits with $0.7 \leq |V_\parallel/V_T| \leq 0.95$. These orbits are highly inclined with respect to Earth's equatorial plane.

Our secondary recommendation, which must be qualitative due to the limited data set from the PDP free-flight mission, is that orbiter-based experiments involving plasma waves should be performed outside and upstream from the orbiter's water cloud and water ion trail so as to avoid confusion with the wide variety, large spectral width, and significant levels of orbiter-associated plasma waves. A similar recommendation follows for other orbiting platforms, such as the proposed space station, which are inhabited or suffer significant outgassing. The PDP free-flight data and theoretical extent of the shuttle orbiter's water cloud [*Paterson and Frank*, 1989] indicate that upstream distances of at least 400 m should be chosen, thereby arguing strongly for such research to be performed using independent, free-flying spacecraft.

7. Conclusions

The plasma wave receiver on the PDP spacecraft observed "mushroom" spectral features with accompanying amplitude enhancements during the free-flight portion of the Spacelab 2 mission. The top of a mushroom feature is formed by a band of lower hybrid frequency waves, while the base of the mushroom is formed by low-frequency waves whose frequency bandwidth increases to meet the lower hybrid frequency band at the apex of the mushroom. The lower hybrid band shows little change during the mushroom feature. Our interest here is primarily in the significant intensity (by a factor of order 10) and bandwidth variations (by a factor of order 10 again) of the low-frequency waves. These mushroom spectral features are centered near times when the shuttle orbiter's velocity (relative to the ionospheric plasma) is perpendicular to the ionospheric magnetic field, i.e., $V_\parallel/V_T$ is small, and when the PDP is downstream from the orbiter. These features are not associated with the orbiter's plasma wake or with the effects of thruster firings or water dumps. The near zone plasma waves observed in the near vicinity of the orbiter also show major changes in amplitude and spectral characteristics with $V_\parallel/V_T$ (Cairns and Gurnett, submitted manuscript, 1990); times of low wave amplitude have $|V_\parallel/V_T| \geq 0.5$.

The existence of a $V_\parallel/V_T$ effect for the waves is strong evidence that the waves are driven by water pickup ions associated with the shuttle orbiter. Two mutually compatible interpretations exist, one in terms of the optimum conditions for wave growth driven by pickup ions, and one in terms of the pickup instability driving the waves. In the first interpretation, maximum growth lengths for the waves are envisaged when the orbiter moves perpendicular to the magnetic field since water ions produced by charge exchange of outgassed water molecules move in the same plane and have the same gyrocenter velocity as the ionospheric plasma and the convected (and growing) plasma waves. In contrast, when the orbiter velocity has a significant component along the magnetic field, the pickup ions and ionospheric plasma (and the plasma waves) move in different planes with significantly different gyrocenter velocities; spatial inhomogeneities in the properties of the water ion distributions driving the waves and the finite size of the orbiter's water cloud then imply a significant limitation of the growth length available for the waves. The second interpretation follows from the mechanism of the pickup instability driving the waves: the instability is driven by the ring speed or beam speed $V_\perp$ of the pickup ions; decreasing the speed $V_\perp$ causes a decrease in the growth rate of the waves with no growth possible below some threshold value of $V_\perp$.

A linear instability theory has been constructed for growth of waves driven by the ring and beam distributions of water ions expected near the space shuttle due to charge exchange. This theory predicts the generation of Doppler-shifted lower hybrid waves in the frequency band of the low-frequency component of the mushroom features. These waves have large growth rates and have wavelengths capable of being detected by the PDP antenna. The theory suggests that variations in the distances available for growth and/or variations in the ring/beam speed $V_\perp$ should permit waves to grow to larger amplitudes over a larger range of wave vectors and so naturally (due to the varying Doppler shift) produce a broader frequency spectrum of waves, thereby explaining the observed $V_\parallel/V_T$ effect. The available observational data appear to favor ring distributions as the source of instability for the observed waves. The waves are then predicted to be generated throughout the region populated with water ions produced in the orbiter's water cloud (the so-called water ion trail). At this stage the waves observed near the lower hybrid frequency appear to have no interpretation in terms of the linear theory developed in this paper. Further work on the linear theory and simulations are required before the theory suggested here may be regarded as an adequate explanation for the plasma waves comprising the mushroom spectral features (or other orbiter-associated waves). In particular, inhomogeneity effects must be considered in detail due to their essential role in the theory, and nonlinear effects may have some influences on the observed spectrum of waves. Nevertheless, the homogeneous linear theory developed here provides considerable support for the interpretation of the mushroom spectral features advanced, and so for the resulting implications for further research on plasma waves in the vicinity of orbiting platforms.

This work has significant implications for the orbits of future shuttle missions and space platforms subject to outgassing that are intended for ionospheric research or active space experiments involving plasma waves: to avoid confusion with the orbiter-associated waves discussed in this paper, (1) the orbit should have $0.7 \leq |V_\parallel/V_T| \leq 0.95$, thereby favoring more nearly polar orbits and arguing strongly against equatorial orbits, and/or (2) the research should be performed using free-flying spacecraft situated well upstream of the orbiter- or platform-associated water ion trail and associated plasma waves.

Acknowledgments. We acknowledge the financial support of NASA grant NAGW-1488 from NASA Headquarters and NASA grant NAG 3-449 with NASA/Lewis Research Center. Helpful discussions with J. S. Pickett concerning the PDP's free-flight mission are also gratefully acknowledged.

The Editor thanks Associate Editor J. U. Kozyra for handling the review process on this paper and M. K. Hudson and T. Neubert for their assistance in evaluating this paper.

REFERENCES

Boardsen, S. A., D. A. Gurnett, and W. K. Peterson, Double-peaked electrostatic ion cyclotron harmonic waves, *J. Geophys. Res.*, *95*, 10,591, 1990.

Bush, R. I., G. D. Reeves, P. M. Banks, T. Neubert, P. R. Williamson, W. J. Raitt, and D. A. Gurnett, Electromagnetic fields from pulsed electron beam experiments in space: Spacelab-2 results, *Geophys. Res. Lett.*, *14*, 1015, 1987.

Cairns, I. H., Transition from ring to beam arc distribution functions of water ions with distance upstream from the space shuttle orbiter, *J. Geophys. Res.*, *95*, 15,167, 1990.

Carignan, G. R., and E. R. Miller, Mass spectrometer STS-2, -3, -4 induced environment contamination monitor (IECM) summary report, edited by E. R. Miller, *NASA Tech. Memo.*, *NASA TM-82524*, 87, 1983.

Coroniti, F. V., C. F. Kennel, F. L. Scarf, E. J. Smith, B. T. Tsurutani, S. J. Bame, M. F. Thomsen, R. Hynds, and K. P. Wenzel, Plasma wave turbulence in the strong coupling region at comet Giacobini-Zinner, *Geophys. Res. Lett.*, *13*, 869, 1986.

Farrell, W. M., D. A. Gurnett, P. M. Banks, R. I. Bush, and W. J. Raitt, An analysis of whistler mode radiation from the Spacelab 2 electron beam, *J. Geophys. Res.*, *93*, 153, 1988.

Gary, S. P., and N. Omidi, The ion-ion acoustic instability, *J. Plasma Phys.*, *37*, 45, 1987.

Grebowsky, J. M., H. A. Taylor, Jr., M. W. Pharro III, and N. Reese, Thermal ion perturbations observed in the vicinity of the space shuttle, *Planet. Space Sci.*, *35*, 501, 1987.

Gurnett, D. A., W. S. Kurth, J. T. Steinberg, P. M. Banks, R. I. Bush, and W. J. Raitt, Whistler-mode radiation from the Spacelab-2 electron beam, *Geophys. Res. Lett.*, *13*, 225, 1986.

Gurnett, D. A., W. S. Kurth, J. T. Steinberg, and S. D. Shawhan, Plasma wave turbulence around the shuttle: Results from the Spacelab-2 flight, *Geophys. Res. Lett.*, *15*, 760, 1988.

Hudson, M. K., and I. Roth, Simulations of active ion injection experiments on ARCS 3, *J. Geophys. Res.*, *93*, 8768, 1988.

Hunton, D. E., and J. M. Calo, Low energy ions in the shuttle environment: Evidence for strong ambient-contaminant interactions, *Planet. Space Sci.*, *33*, 945, 1985.

Hwang, K. S., N. H. Stone, K. H. Wright, Jr., and U. Samir, The emissions of broadband electrostatic noise in the near vicinity of the shuttle orbiter, *Planet. Space Sci.*, *35*, 1373, 1987.

Kurth, W. S., and L. A. Frank, The Spacelab-2 Plasma Diagnostics Package, *J. Spacecr. Rockets*, *27*, 70, 1990.

Lee, J. K., and C. K. Birdsall, Velocity space ring-plasma instability, magnetized, I, Theory, *Phys. Fluids*, *22*, 1306, 1979.

Murphy, G. B., S. D. Shawhan, L. A. Frank, N. D'Angelo, D. A. Gurnett, J. M. Grebowsky, D. L. Reasoner, and N. Stone, Interaction of the space shuttle orbiter with the ionospheric plasma, Spacecraft/Plasma Interactions and Their Influence on Field and Particle Measurements, *Eur. Space Agency Spec. Publ.*, *ESA SP-198*, 73, 1983.

Murphy, G. B., D. L. Reasoner, A. Tribble, N. D'Angelo, J. S. Pickett, and W. S. Kurth, The plasma wake of the shuttle orbiter, *J. Geophys. Res.*, *94*, 6866, 1989.

Narcisi, R., E. Trzcinski, G. Federico, L. Wlodyka, and D. Delorey, The gaseous and plasma environment around space shuttle, *AIAA Pap.*, *83-2659*, 1983.

Neubert, T., G. D. Reeves, J. G. Hawkins, P. M. Banks, R. I. Bush, P. R. Williamson, W. J. Raitt, and D. A. Gurnett, Pulsed electron beam emissions in space, *J. Geomagn. Geoelectr.*, *40*, 1221, 1988.

Papadopoulos, K. D., On the shuttle glow (the plasma alternative), *Radio Sci.*, *19*, 571, 1984.

Paterson, W. R., and L. A. Frank, Hot ion plasmas from the cloud of neutral gases surrounding the space shuttle, *J. Geophys. Res.*, *94*, 3721, 1989.

Pickett, J. S., N. D'Angelo, and W. S. Kurth, Plasma density fluctuations observed during space shuttle orbiter water releases, *J. Geophys. Res.*, *94*, 12,081, 1989.

Reeves, G. D., P. M. Banks, T. Neubert, R. I. Bush, P. R. Williamson, A. C. Fraser-Smith, D. A. Gurnett, and W. J. Raitt, VLF wave emissions by pulsed and DC electron beams in space, 1, Spacelab 2 observations, *J. Geophys. Res.*, *93*, 14,699, 1988.

Shawhan, S. D., Description of the Plasma Diagnostics Package (PDP) for the OSS-1 shuttle mission and JSC chamber test in conjunction with the fast pulse electron gun (FPEG), in *Artificial Particle Beams in Space Plasma Studies*, edited by B. Grandel, p. 419, Plenum, New York, 1982.

Shawhan, S. D., G. B. Murphy, and J. S. Pickett, Plasma Diagnostics Package initial assessment of the shuttle orbiter plasma environment, *J. Spacecr. Rockets*, *21*, 387, 1984.

Stone, N. H., U. Samir, K. H. Wright, Jr., D. L. Reasoner, and S. D. Shawhan, Multiple ion streams in the near vicinity of the space shuttle, *Geophys. Res. Lett.*, *10*, 1215, 1983.

Tataronis, J. A., and F. W. Crawford, Cyclotron harmonic wave propagation and instabilities, I, Perpendicular propagation, *J. Plasma Phys.*, *4*, 231, 1970.

Tribble, A. C., J. S. Pickett, N. D'Angelo, and G. B. Murphy, Plasma density, temperature, and turbulence in the wake of the shuttle orbiter, *Planet. Space Sci.*, *37*, 1001, 1989.

I. H. Cairns and D. A. Gurnett, Department of Physics and Astronomy, University of Iowa, Iowa City, IA 52242.

(Received April 6, 1990;
revised October 29, 1990;
accepted November 13, 1990.)